MMA Memo 246

Optimized Optical Layout for MMA 12-m Antennas

James W Lamb

Abstract— **We discuss the criteria affecting the choice of optical configuration for the MMA antennas. Receiver bands will be separated in the focal plane so the selection of Cassegrain parameters is influenced by the acceptable size and separation of the feeds and the associated aberrations. The secondary mirror size is determined by blockage restrictions and by nutation requirements. Specifications for the nutation of the secondary need to be carefully considered since the dynamics and aberrations are very strongly influenced by beam-throw and nutation frequency requirements. A set of design parameters is derived which is a reasonable compromise among the various constraints.**

I. Introduction

With the decision to build 12-m antennas we need to revise the optical parameters for the antenna Request for Proposal. Some of the dimensions may need to be iterated on with the antenna manufacturer so we present here the relevant points which need to be considered. On the basis of these we can limit the parameter space and recommend an optimum starting geometry.

The Cassegrain geometry is defined by four parameters (Section II). In choosing these we need to consider the implications on the RF performance (field of view, blockage, spillover) and the structure (receiver location, secondary support stiffness, nutating secondary dynamics). The RF performance should ultimately be evaluated by G/T, where G is the antenna gain, and T is the system temperature.

The current plan assumes that the antenna is a conventional design (*i.e.*, not shaped for uniform illumination). This is essentially imposed by the wish to have the different receiver bands share the focal plane so that selecting the receiver band requires simply re-pointing the antenna [1]. Aberrations related to these off-axis feeds are dealt with in Section III. If array receivers are installed in the future the same considerations will apply.

Diffraction effects at the secondary, including efficiency loss and spillover, are covered in Section IV.

The prototype antenna will have a nutating secondary for single dish total power measurements—a decision will be made later whether or not to equip all antennas in the array. Tradeoffs between the optical and mechanical constraints are discussed in Section V.

15 January 1999
Owens Valley Radio Observatory, California Institute of Technology, Big Pine, CA 93513, USA

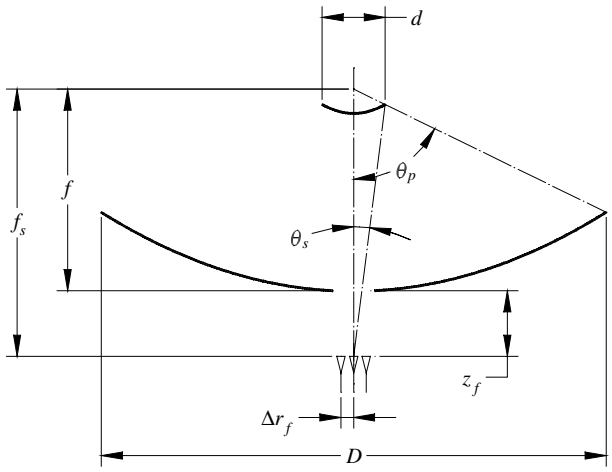

Fig. 1. Parameters for Cassegrain geometry as used in the text. The different receiver bands are separated in the focal plane.

II. Antenna Parameters

We will choose the following four parameters to define the Cassegrain geometry (Fig. 1):

Primary mirror diameter, D

Primary focal length, f

Secondary mirror diameter, d

Magnification, M

Other parameters may be derived from these as follows:

Primary focal ratio, f/D

Focal length of equivalent paraboloid, $F = Mf$

Secondary focal ratio, F/D

Eccentricity of secondary, $e = \dfrac{M+1}{M-1}$

Secondary mirror interfocal distance,

$$f_s = \frac{d(M+1)(16f^2M - D^2)}{16MDf}$$

Distance of secondary focus behind primary (back focal distance), $z_f = f_s - f$

Half-angle subtended by primary, $\theta_p = 2\ \mathrm{atan}(D/4f)$

Half-angle subtended by secondary, $\theta_s = 2\ \mathrm{atan}(D/4f)$

We will assume that the antenna diameter is fixed at 12 m. The remaining parameters should be determined with the following considerations in mind.

Primary focal length: Close packing of antennas; stiffness and resonances of the secondary mirror support; aberrations.

Secondary diameter: Aberrations; location of focus (and receivers); dynamical requirements for nutation; weight at prime focus; blockage, efficiency and spillover losses due to edge diffraction.

Magnification: Aberrations; focal plane plate scale (spot size, physical layout of receivers); location of focus.

III. Off-Axis Feed Aberrations

Padman [2] gives some useful expressions for the aberrations in the focal plane of a Cassegrain antenna. The principal effects are coma, astigmatism and field curvature. Using the expressions for the wavefront errors in [2] we can calculate the effect on aperture efficiency for the corresponding wavefront errors. If a feed is moved off axis a distance Δr_f to give a beam squint on the sky of $\alpha = \Delta r_f / F$, the corresponding fractional reductions in aperture efficiency are

Astigmatism: $$\Delta\eta_{ast} = \left(\frac{\pi D^3}{16 M f d \lambda} \right)^2 \alpha^4 \quad (1)$$

Coma: $$\Delta\eta_{com} = \frac{1}{2}\left(\frac{\pi D^3}{96 M^2 f^2 \lambda} \right)^2 \alpha^2 \quad (2)$$

Curvature: $$\Delta\eta_{cur} = \frac{1}{3}\left(\frac{\pi D^3}{16 f d \lambda} \right)^2 \alpha^4 \quad (3)$$

Uniform aperture illumination was assumed in deriving these equations, so lower losses will result from a tapered aperture field.

Comatic losses rise as the square of the off-axis angle rather than the fourth power and will therefore dominate at small angles. However, we find that for typical values of F and λ, as we increase α the astigmatic and curvature errors exceed the comatic ones when the magnitudes are still small (at the ½% level or less), so coma can generally be neglected. (Note that the aberration given by Padman includes a small pointing offset. (2) includes the pointing correction which reduces the loss by a factor of 9).

Astigmatism and curvature have the same dependence on α and we find the ratio of the loss due to astigmatism to that due to curvature to be $3/M^2$. Although the loss due to curvature will exceed that due to astigmatism for $M >$ ~1.7 the wavefront error due to curvature may be almost completely removed, either by moving the feed forward from the nominal focal plane, or by refocusing the secondary mirror. This will in fact also reduce the astigmatic loss since we can effectively put the feed mid-way between the two line foci. The amount the feed has to be moved in the focal plane can be calculated from the Petzval surface [3]. Since the curvature of the Petzval surface is the sum of the inverse focal lengths of all the focusing elements it is determined principally by the secondary mirror. We find that a good approximation for the radius of curvature of the Petzval surface is

$$R_{Petz} = d\frac{f}{D} \quad (4)$$

For typical primary focal ratios R_{Petz} will therefore be a half to a third of the secondary mirror diameter.

Since the dominant aberration is astigmatism, from (1) we would like to maximize the secondary diameter, the primary focal length, and the magnification. Coma and curvature will also be reduced with longer primary focal lengths, and the coma benefits from a higher magnification.

The size of the feeds will scale with the secondary focal ratio, F/D, as will the feed separation for a given beam squint.

IV. Secondary Mirror Diffraction

Diffraction by the secondary mirror is proportional to the illumination at its edge and the square root of the mirror diameter in wavelengths. For a Gaussian illumination, the expression for diffraction efficiency given by Kildal [4] may be simplified to

$$\eta_d = 1 - 2C_d A_0 \sqrt{\frac{\lambda}{d}} \quad (5)$$

where

$$C_d = \frac{-\ln(A_0)}{\pi(1 - A_0)} \quad (6)$$

and A_0 is the field amplitude at the secondary edge relative to the center. For an edge taper of 12 dB this gives an efficiency reduction of ~2% for a 200 wavelength reflector (*e.g.* 600 mm at 3-mm wavelength). Spillover will be less than half of this. Numerical evaluations for a 750-mm secondary predicted 1 K of diffraction spillover noise at 4 mm wavelength [5].

The diffraction from the edge of the secondary causes the illumination at the primary to have some ripple towards the edge of the aperture [3]. Closer to the rim the illumination drops exponentially and is –6 dB of its geometrical optics value at the edge of the aperture. The scale size of the diffraction pattern at the primary (taken to be the period of the ripple) is about 0.5 m at a wavelength of 3 mm. The decay distance outside the primary (spillover) is on this scale. Adding a skirt outside could put this on cold sky, but a 75% reduction would require a 0.5 m radius skirt. At higher frequencies a smaller skirt could be used, and it may be reasonable to have a 0.3 m shield to reduce the 1-mm spillover by this amount.

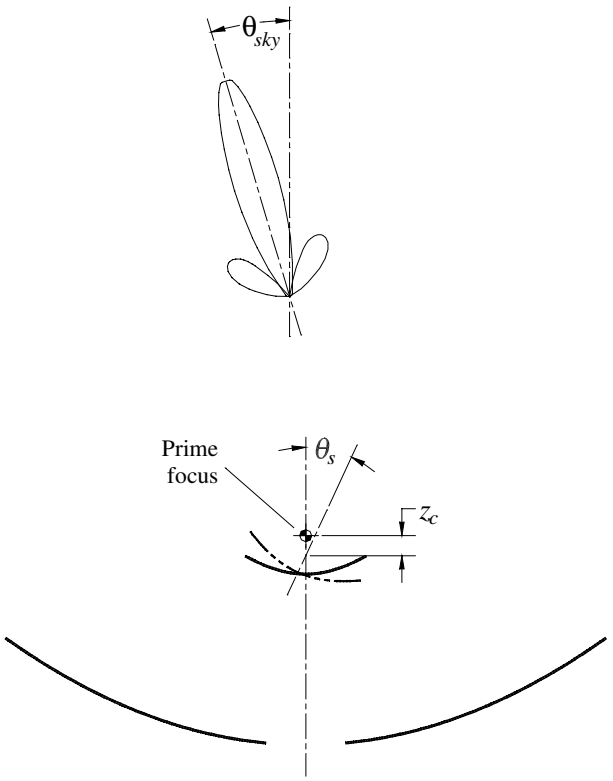

Fig. 2. Geometry and parameters for beamswitching by nutating the secondary mirror.

If the feed is offset or the secondary rotated to tilt the beam, the aperture illumination pattern is displaced on the primary. Typically the distance it is shifted is comparable to the diffraction pattern scale and the change in spillover loss is less than the geometrical calculation would indicate.

Since diffraction loss varies inversely as the square root of the secondary diameter in wavelengths it is not a significant factor in the diameter choice.

V. Secondary Mirror Nutation

Nutation of the secondary mirror may be used to rapidly chop the beam on the sky [6]. For point sources it is necessary to go only about three beamwidths off source, but larger throws are sometimes specified for extended sources. For observing regions much larger than a beamwidth a differential measurement is made [7]. At 3-mm wavelength the beamwidth is about 1 arcmin so that a ±1.5 arcmin throw is sufficient for point sources. The use of beam switching in the test antenna and possibly the array needs to be defined so that appropriate specifications are set.

A. Switching Parameters

Movement of the telescope beam on the sky is produced by rotating the secondary through angle θ_s about an axis that is z_c from the prime focus (Fig. 2). The required secondary tilt for a given angle on the sky, θ_{sky}, is a function of this distance, M, f, and f_s. The ratio of the two is

$$\beta = \frac{\theta_{sky}}{\theta_s} = -\left(\frac{z_c}{f} + \frac{f_s - z_c}{Mf} \right) \tag{7}$$

This is a linear function of z_c, and it has a zero when the center of rotation is at the paraxial center of curvature of the secondary, $-f_s/(M-1)$. Rotation about the prime focus gives $\beta = -f_s/F$.

B. Aberrations

In addition to tilting the aperture wavefront to give the desired beam throw, the rotated secondary produces undesirable aberrations. These are primarily coma and astigmatism. Comatic aberrations (measured as a path error) are proportional to θ_s producing a gain degradation quadratic in θ_s. Astigmatic errors are proportional to θ_s^2 with a gain degradation proportional to θ_s^4. Generally the aberrations are dominated by coma, but when the center of rotation is close to the prime focus the coma due to the secondary virtually cancels the coma due to the primary and the astigmatic term dominates even for small beam throws. Overall aberrations are smallest for this condition.

We have carried out some detailed calculations of the various parameters using ray-tracing to obtain the aperture field. Fig. 3 shows the equivalent surface error (RMS half wavefront error) as a function of the location of the rotation center. Weighting the result by the aperture illumination generally has a relatively minor effect except where astigmatism dominates. This is because the astigmatic errors are greatest at the edge of the aperture where they are given low weighting by the illumination taper.

The effective surface error is comparable to or exceeds the total budget of 25 μm for the antenna. It is a common-mode wavefront error for all antennas, but since it has a large spatial scale and is stable and predictable, it should be

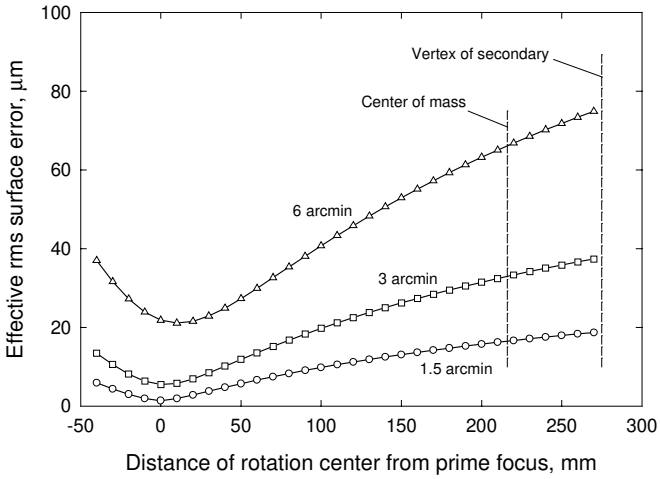

Fig. 3. Effective surface error from aberrations due to rotation of secondary. The curves are labeled with the beam throw on the sky, θ_{sky}. The parameters are f = 4.8 m, d = 750 mm, and M = 20.

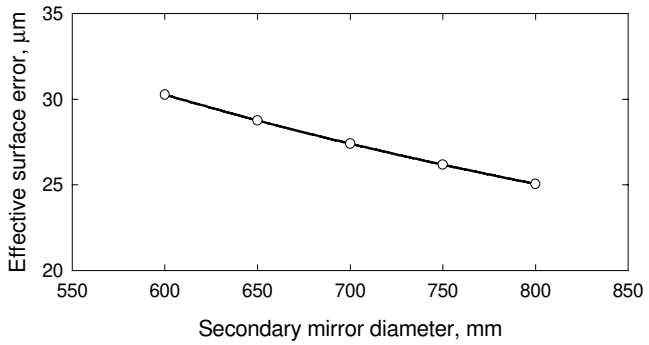

Fig. 4. Dependence on effective surface error on secondary diameter for f = 4.8 m, M = 20, z_c = 150 mm, θ_{sky} = 3 arcmin.

possible to calibrate it out for extended source measurements. For point sources it leads to an inevitable loss of sensitivity.

Fig. 4 shows the influence of secondary diameter on the aberrations for a maximum beam throw of ±3 arcmin. Since the dependence is weak, the diameter of the secondary can be chosen mainly on mechanical considerations.

C. Dynamics

For a given torque, T, the minimum time, t_b, to tilt the secondary through an angle θ_s is given by

$$t_b = 2\sqrt{\frac{I_{tot}\theta_s}{T}} \tag{8}$$

where I_{tot} is the moment of inertia of the secondary and any counterweights. For a given θ_{sky}, θ_s will be found from (7). T will depend on the motor and servo, and I_{tot} on the considerations given below.

We can compute the peak and average power required for the drives. If there is no recovery of power in the braking part of the cycle, the peak power will be

$$P_{pk} = \frac{2I_{tot}\theta_s^2}{t_b^3} \tag{9}$$

while, for a switching frequency of f_{sw}, the average power will be

$$P_{avg} = 4f_{sw}\frac{I_{tot}\theta_s^2}{t_b^2} \tag{10}$$

For a fixed duty-cycle, $(2f_{sw}t_b)^{-1}$, the average power is proportional to ${f_{sw}}^3$.

D. Moments of Inertia

The intrinsic moment of inertia of the secondary, I_{s0}, depends on its geometry, material, and diameter. For a given design, a linear scaling of all the dimensions changes the moment of inertia according to

$$I_{s0} \propto d_s^5 \tag{11}$$

indicating the importance of using a small diameter. If the center of rotation is not coincident with the center of mass the moment of inertia will be

$$I_s = I_{s0} + r_s^2 m_s \tag{12}$$

where m_s is the mass of the secondary and r_s the distance of the center of rotation from the center of mass. There is therefore some penalty for moving the rotation center away from the center of mass of the secondary. In addition, a counterweight is required for static balancing of the mirror[1]. The counterweight will have a smaller moment of inertia than the secondary, and it will add proportionally to the drive requirement. The moment of inertia of the counterweight around the rotation axis is

$$I_{cw} = I_{cw0} + r_{cw}^2 m_{cw} \tag{13}$$

where r_{cw} is the distance of mass m_{cw} from the rotation axis, and I_{cw0} is moment of inertia of the counterweight about is center of mass. The mass is found from

$$m_{cw} = m_s r_{cw} / r_s \tag{14}$$

For large r_{cw} the second term dominates in (13). As r_{cw} is decreased the second term drops but I_{cw0} increases, so that (13) has a minimum for some value of r_{cw}. Using the expressions for a sphere of density ρ leads to the analytical

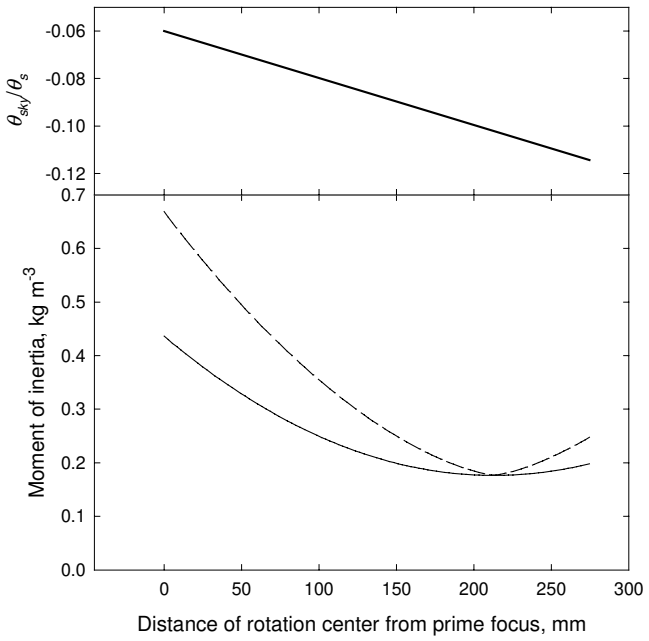

Fig. 5. Total moment of inertia about a point z_c from the prime focus for the secondary mirror (solid line), and the mirror plus counterbalance (dashed line). The upper graph gives the corresponding factor for the ratio of sky tilt to secondary mirror tilt. Parameters are given in the text.

[1] "Static balance" is used to mean that there are no net reaction forces on the support when the reflector is chopped. "Dynamic balance" implies that there are no residual torques.

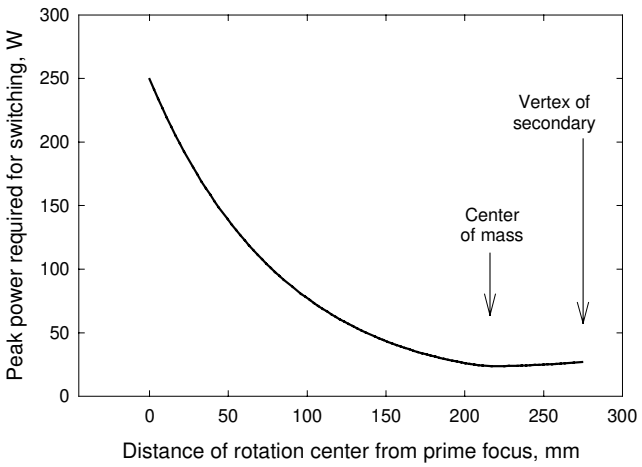

Fig. 6. The peak power needed to drive the secondary for a throw of ±1.5 arcmin at 5 Hz rate with a 10% duty-cycle. The average power is a tenth of this.

result that

$$I_{cw,\min} = 0.96(m_s r_s)^{1.25} \rho^{-0.25} \tag{15}$$

The optimum value will typically result in an increase of the moment of inertia of up to ~60% over the secondary alone.

Nutating at high frequencies and beam throws may demand that the secondary is dynamically balanced, which will double the inertia and drive power requirements.

As an example we consider a 750-mm diameter mirror with a mass of 5.7 kg and an intrinsic moment of inertia of 0.175 kg m^2. These are in fact low values, but still feasible. Fig. 5 illustrates how the moment of inertia of the secondary varies with z_c. Also shown is the inertia for the mirror plus an optimum static balance counterweight. Compared to nutation about the center of mass, we find that the moment is more than doubled when we tilt around the prime focus. Furthermore, β increases by ~50%. Both effects contribute to an increase in the drive requirements. From the plot of peak required drive power (Fig. 6) we see that the minimum is not for rotation about the center of mass but for an axis shifted towards the vertex, since β is reduced. The average power is ten percent of the peak for a 95% duty-cycle. As an extreme case, for $z_c = 0$, $t_b = 10$ ms, and $\theta_{sky} = \pm 6$ arcmin, the peak power required jumps to 4 kW!

It is clearly very important to decide on the nutation frequency, duty-cycle, and beamthrow to finalize the decision on optics. We recommend switching close to the center of mass at a switching rate of 5 Hz or less and 90% duty-cycle, and statically but not dynamically balancing the mirror.

VI. Choice of Parameters

We can now try to determine an optimum set of parameters from the above arguments. Since the primary focal length does not have a strong influence on the performance we will take a value of 4.8 m giving a primary focal ratio of 0.4. This is appropriate for the OVRO antenna design [8] and is consistent with close packing of antennas. Note that longer focal lengths help to reduce aberrations. In particular the astigmatic losses which are the most significant limit are reduced as the square of the focal length.

The magnification and diameter of the secondary will then be driven by all the considerations of the previous sections. There are two other physical constraints, which should be added. We would like to specify that the receivers are behind the primary vertex by an amount z_f. Furthermore, we would like to prescribe a maximum off-axis distance for the feeds to limit the size of the hole in the primary, and more importantly for a large antenna, the size of the dewar.

At the secondary focus the effective focal ratio determines the focal spot size and the feed offset for a given beam squint. We can assume that there is some arrangement of feeds in the focal plane which accommodates all the bands (*e.g.*, as given in [1]) and can be scaled linearly with the focal spot size. The receiver size then scales with the focal ratio. There is no particular lower limit for the focal ratio from this, but at high *f*-numbers the windows in the dewar become large. Since the minimum window thickness increases as the second or third power of the area for a given strength, the dielectric losses (at room temperature) become serious. (We can use re-imaging optics to get around this, which will be discussed in a later Memo.)

Following d'Addario [9], let the diameter of the window in the dewar be

$$w = 5\lambda F / D \tag{16}$$

and also let the dewar diameter be

$$d_{dewar} = 3w_{\max} \tag{17}$$

(*c.f.* [1]). w_{max} is the window size at the longest wavelength which we take to be 4 mm. Putting requirements that w < 160 mm and d_{dewar} < 600 mm gives us *f*-numbers of <8 and <10 respectively.

The requirement of having the receivers and therefore secondary focus a distance z_f behind the secondary means that

$$d > \frac{f + z_f}{F / D} \tag{18}$$

giving d > 725 mm for $F/D = 8$ and $z_f = 1$ m. Minimizing aberrations also favors a larger secondary diameter.

Upper limits on the secondary diameter come from the nutation and blockage requirements. If we specify an effective blockage area of <1% for a 12 dB Gaussian taper then the secondary diameter should be less than 850 mm. As discussed in Section V, the high power dependence on diameter of the dynamics of a nutating secondary require minimizing the size.

From the above considerations, the parameters shown in Table I are recommended for the 12-m antennas.

The maximum window size using (16) is then 160 mm at a wavelength of 4 mm. The dewar diameter would be ~480 mm from (17), so that the outermost feed would be centered 200 mm off axis. The Petzval surface at this off-axis distance is about ~80 mm above the nominal focal plane. The

feed could be located there or, the secondary mirror could be refocused by $1/M^2$ of this (~0.2 mm).

However, if we arrange to have the lowest band at the edge of the dewar the wavefront curvature loss will be < 1% *without* refocusing for frequencies less than 120 GHz. The shorter wavelength bands would be closer to the optical axis and the loss reduced in proportion to $1/\lambda^2\Delta r_f^4$. This is more favorable than the arrangement in [1], which for which the curvature loss would have been very significant [10]. In practice, the antenna would be focused for the band being observed, and the small losses at the low-frequency band used for phase calibration would be tolerable.

The 33-45 GHz observing band and potentially a 22 GHz water vapor radiometer band have not been considered explicitly. The former would most easily be incorporated with a mirror that could be switched in front of the other optics. A 22 GHz water vapor radiometer would be much harder to accommodate than a 183 GHz one. However it could be located beside the main dewar with a mirror to bring the beam as close to the axis as possible. The aberrations would not affect the performance, but a major problem is the size of the feed. Using the criterion in (16) results in a system with a 500-mm diameter focusing mirror. If the hole in the primary is smaller than the secondary mirror there will be only 135 mm outside the circle enclosing the observing band feeds. It is probable that it could overlap some part of this circle, but would still necessitate enlargement of the central hole by about 200 – 400 mm on one side.

TABLE I: PARAMETERS FOR CASSEGRAIN ANTENNA

Parameter	Symbol	Value
Primary diameter	D	12.00 m
Primary focal length	F	4.8 m
Secondary diameter	d	750 mm
Magnification	M	20
Secondary eccentricity	e	1.10526
Equivalent focal length	F	96.00 m
Primary focal ratio	f/D	0.40
Secondary focal ratio	F/D	8.00
Secondary interfocal length	f_s	6.177 m
Half-angle of primary	θ_p	64.01°
Half-angle of secondary	θ_s	3.58°
Back focal distance	z_f	1.38 m
Radius of Petzval surface	R_{petz}	300 mm
Rotation center for secondary	z_c	150 mm
Beam throw	θ_{sky}	±1.5 arcmin
Beamswitch frequency	f_{sw}	5 Hz
Blanking time	t_b	10 ms

VII. CONCLUSIONS

The optical parameters of the Cassegrain have been determined on the basis of focal plane aberrations, focal spot size, blockage, and feasibility of implementing a nutating secondary. The secondary diameter has a maximum size of 850 mm based on a 1% effective area blockage. The requirement of not having too large a focal spot and correspondingly large dewar window, combined with a need to place the receivers some distance behind the primary effectively limit the smallest secondary diameter to 725 mm. Within this range there is some latitude for variation according to other criteria. Nutation of the secondary is one which is made significantly easier for small diameters. Other criteria such as edge diffraction are minor considerations.

A diameter of 750 mm seems to best satisfy these points. If the secondary nutation is not likely to be incorporated in the final array antennas then the size may be increased. This would allow the dewar window diameter to be reduced (for the same receiver location). If the secondary position is kept fixed, Md will be roughly constant so that astigmatism remains unchanged. Coma will increase, but still be acceptably low, and curvature loss will be reduced. Diffraction loss and spillover are also slightly less.

ACKNOWLEDGEMENTS

I would like to thank John Payne for checking many of the calculations and equations. Peter Napier and David Woody also made some useful suggestions on the content.

REFERENCES

[1] J. Lugten and J. Welch: "A suggested receiver layout for the MMA antenna," Memo 183, NRAO MMA Memo Series, Sep. 1997.

[2] R. Padman: "Optical fundamentals for array feeds," *Multi-Feed Systems for Radio Telescopes*, (D. T. Emerson and J. M. Payne, Eds), ASP Conference Series, vol. 7, 1995.

[3] M. Born and E. Wolf: *Principles of Optics*, Oxford: Pergamon Press, 1980.

[4] P-S. Kildal: "The effects of subreflector diffraction on the aperture efficiency of a conventional Cassegrain antenna—An analytical approach," *IEEE Trans. Antennas Propagat*., vol. AP-31, no. 6, pp. 903-909, Nov. 1983.

[5] J. W. Lamb and A. D. Olver: "Gain loss and noise temperature degradation due to subreflector rotations in a Cassegrain antenna," *Proc. Int. Conf. Antennas Propagat. 85*, April 1985.

[6] J. M. Payne: "Switching subreflector for millimeter wave radio astronomy," Rev. Sci. Instrum., vol. 47, pp. 222-223, 1976.

[7] D. T. Emerson, U. Klein, and C. G. T. Haslam: "A multiple beam technique for overcoming atmospheric limitations to single-dish observations of extended radio sources," *Astron. Astrophys.*, vol. 76, pp. 92-105, 1979.

[8] D. Woody and J. Lamb: "Yet another design for MMA antennas," Internal Memo., March 1998.

[9] L. d'Addario, E-Mail Memo, November, 1998.

[10] B. Shillue: "Gain degradation in a symmetrical cassegrain antenna due to laterally offset feeds," Memo 175, NRAO MMA Memo Series, Jun. 1997.